

Projection of Storm Surge Climate Extreme over Sunda Shelf Based on IPCC SRES A2 Scenario

(Unjuran Iklim Melampau Pusuan Ribut di Pentas Sunda Berdasarkan Senario IPCC SRES A2)

WAH SHIN HOW, HALIMATUN MUHAMAD, FREDOLIN T. TANGANG & LIEW JUNENG*

ABSTRACT

The historical and future storm surge climate over the South China Sea Sunda Shelf was derived using a barotropic two dimensional model. The atmospheric forcings were obtained from the UKMO regional climate modeling system, PRECIS (Providing Regional Climates for Impacts Studies), forced at the boundary by the ECHAM4 simulation output under the SRES A2 emission experiment. In general, the model simulates historical sea surface elevation characteristics satisfactory although there is a substantial underestimation for the sea level elevation at local scales. The climate change analysis suggests that the storm surge extreme over the Sunda Shelf is expected to increase along the coastal area of the Gulf of Thailand and east coast of Peninsular Malaysia in the future (2071-2100). The projected increment is averagely ~9% over the Sunda Shelf region by the end of the 21st century corresponding to about 5% stronger wind speed as compare to the baseline period of 1961-1990.

Keywords: Climate change; Princeton Ocean Model; sea level elevation; storm surge; Sunda Shelf

ABSTRAK

Iklim pusuan ribut pada masa lampau dan masa depan di Laut China Selatan telah diterbitkan dengan menggunakan model lautan barotropik berdimensi dua. Pendayaan atmosfera didapati daripada sistem model iklim serantau UKMO PRECIS (Providing Regional Climates for Impacts Studies) yang dipacu dengan hasil simulasi ECHAM4 pada sempadan model di bawah eksperimen senario emisi masa depan SRES A2. Secara amnya, model ini berjaya mensimulasikan ciri-ciri ketinggian permukaan laut masa lampau walaupun model ini menganggar magnitud ketinggian permukaan laut yang lebih kecil pada skala tempatan. Dalam analisis perubahan iklim, iklim melampau pusuan ribut pada masa depan (2071-2100) di Laut China Selatan dijangka akan meningkat di sepanjang kawasan pantai Teluk Thailand dan juga pantai timur Semenanjung Malaysia. Secara puratanya, peningkatan yang diunjur di Pentas Sunda adalah kira-kira 9% pada akhir abad ke-21 sebagai tindak balas terhadap penambahan kelajuan angin kira-kira 5% berbanding dengan masa lampau iaitu tempoh masa dari tahun 1961 hingga 1990.

Kata kunci: Ketinggian permukaan laut; Model Laut Princeton; Pentas Sunda; perubahan iklim; pusuan ribut

INTRODUCTION

The storm surge is a regional coastal phenomenon where the sea level elevation is above or below the predicted tide level caused by several combined forcings, such as strong atmospheric wind, low atmospheric pressure and continental-trapped waves along the coast (Bell et al. 2000; Gönner 2004). Flood and inundation induced by storm surge events are major threats to the populated areas adjacent to coastal margin and low lying areas along the coastline of South China Sea Sunda Shelf. For instances, Typhoon Linda in 1997, generated surge height of approximately 1.0-2.5 m along the coastline of Gulf of Thailand. This phenomena has caused over 330 deaths and approximately 2,250 people missing in the coastal areas of Thailand and Vietnam (Ascharyaphotha et al. 2011; Wannawong et al. 2010).

There is a concern on the diversification of storm surge characteristics along the coastal areas under the

effect of global warming (von Storch & Woth 2008). Based on the Intergovernmental Panel on Climate Change Fourth Assessment Report (IPCC AR4) (2007), the storm frequency and intensity is projected to increase globally in the future. The increment of storm frequencies and intensity is expected to modify the characteristics of storm surge with substantial regional and temporal variations. For instances, over the North Sea and the Norwegian Sea, the storm surge extreme is expected to be increased by ~10% (Woth et al. 2006). Debernard et al. (2002) argues that surge height increment is the greatest during the autumn over the southwest part of the North Sea. On the other hand, Lionello et al. (2003) reports no significant surge height climate changes over the Adriatic Sea with the doubling of CO₂ in future climate. Over the Australian regions, Pittcock et al. (1996) expected an increment of coastal inundation due to combine effect of mean sea level rise of 0.8 m with the increment of 10% wind forcing under

the warmer climate. In general, the changes of storm surge characteristics are region dependent and associate to local atmospheric conditions and coastal morphologies.

The Sunda Shelf region of the South China Sea is one of the susceptible regions to the meteorological disturbances dominated by strong monsoon influence. The surface atmospheric conditions are expected to be altered significantly by the changing climate due to the increasing greenhouse gases. Both observational and modeling studies had indicated potential strengthening of surface winds over the regions (Hori & Ueda 2006; Hu et al. 2000; Juneng & Tangang 2010). In addition, with the essential recipes including the shallowness and wideness, the Sunda Shelf has favorable conditions for generation of high surge elevation (Ascharyaphotha et al. 2011). Hence, simulation and projection of storm surge are the basis for coastal adaptation to future climate change coastal impact at this region.

Numerous studies on the projection of future storm surge climate under the global warming scenarios have been conducted by using different hydrodynamic models. In the North Sea region, Lowe et al. (2001) used a tide-surge model to study the storm surge activity. In the same region, a barotropic tide-surge model, TRIMGEO, was used by Woth et al. (2006) to derive storm surge climate driven by dynamically downscaled data from different regional climate models (RCMs). Kolomiets et al. (2010) used 2D shallow water, finite volume model - COASTOX-UN for future storm surge downscaling experiment over the Singapore Strait. In current study, a 2D barotropic model is used to derive future storm surge climate over the South China Sea Sunda Shelf based on the IPCC SRES A2 emission scenario.

DATA AND METHODOLOGY

DATA

The flow charts of the downscaling procedures is shown in Figure 1. The downscaling of low resolution global climate model (GCM) output to a fine resolution of $0.44^{\circ} \times 0.44^{\circ}$ was performed by using the Hadley Centre's regional climate model - Providing Regional Climates for Impacts Studies (PRECIS) (Rupa Kumar et al. 2006; Wilson et al. 2009). The high resolution downscaled atmospheric data is crucial to be used as input to the storm surge model in order to reproduce mesoscale features of the coastal processes. Three sets of atmospheric forcing were used: one set for hindcast and two sets for scenario simulations. In the hindcast (HIND) simulation, 30-year downscaled ERA40 (ECMWF Re-Analysis 40) surface wind and sea level pressure were obtained from PRECIS output covering 1961-1990. The hindcast simulation outputs were used for validation purpose. The quality of the hindcast simulation was examined via the comparison of the model output with the station observed data.

In addition, two simulations in the climate change scenario experiment; the baseline simulation (BL) (1961-1990) and the future simulation (2071-2100) are used to obtain the future storm surge climate changes under the increasing green house gases based on the IPCC SRES A2 scenario. The SRES A2 scenario represents a heterogeneous world with continuous increment of world population, fragmented technology change and regional economic development. The concentration of CO_2 increases from about 350 ppm to 850 ppm at the end of the 21st century (2000-2099) (Sheffield & Wood 2008). The downscaling

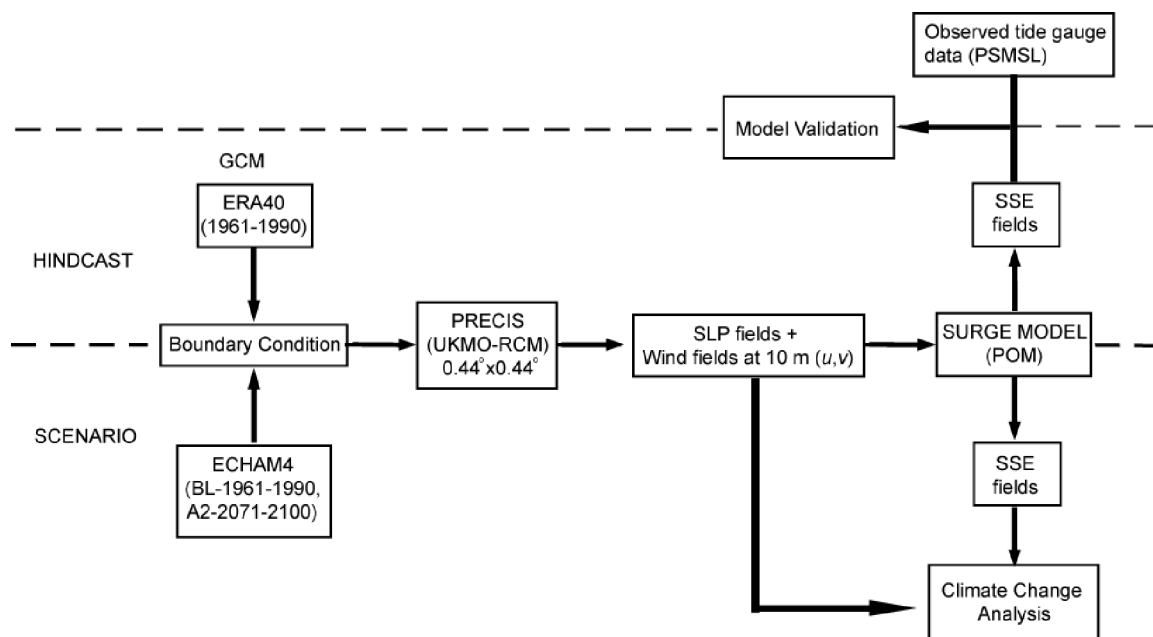


FIGURE 1. The procedure of the study. Global circulation output acts as the boundary condition for the regional model, PRECIS. The downscaled output used as atmospheric forcings for the surge model to produce SSE

for the climate change experiment was driven by the MPI ECHAM4 GCM.

The atmospheric forcing data from PRECIS was interpolated bilinearly to finer grids of the storm surge model ($0.1^\circ \times 0.1^\circ$). The surface kinematic wind stress field was computed from the 10 m zonal and meridional wind (u, v) using equation (1) to force the storm surge model:

$$\begin{bmatrix} \tau_x \\ \tau_y \end{bmatrix} = \rho' C_{drag} \sqrt{u^2 + v^2} \begin{bmatrix} u \\ v \end{bmatrix}, \quad (1)$$

where τ_x and τ_y are the corresponding kinematic wind stress for zonal and meridional wind, respectively; $\rho' = \frac{\rho_{air}}{\rho_{water}}$ where ρ_{air} is the air density and ρ_{water} is the water density; C_{drag} is the drag coefficient.

For storm surge simulation validation, observed hourly sea level data from six tide monitoring stations (Figure 2) was extracted from the Permanent Service for Mean Sea Level (PSMSL), based at the National Oceanography Centre, Liverpool (PSMSL 2010). The stations were chosen to determine how well the model is able to simulate sea surface elevation at different morphologies and locations of the broad region, covering the southern South China Sea. The geographical information of the chosen stations is provided in Table 1.

THE STORM SURGE MODEL

Princeton Ocean Model (POM) (Blumberg & Mellor 1983) was implemented to simulate and project the storm surge climate extreme in this study. Ascharyaphohta et al. (2011) demonstrated reasonable performance of POM in simulating surge height induced by the Typhoon Linda over the Gulf of Thailand. Other studies modified the POM model code to simulate storm surge climate in their specific regions (Bernier & Thompson 2006; Debernard et al. 2002; Peng et al. 2006).

In the current study, POM was configured to run in two dimensional barotropic mode to solve the shallow water equations for the sea surface elevation (SSE) and depth averaged circulations (Mellor 2004). The two dimensional

configuration of the POM model has been used in studying the Indonesian Seas circulation (Burnett et al. 2000) and in various storm surge experiments in Gulf of Thailand (Ascharyaphohta et al. 2011; Wannawong et al. 2010). The model domain comprises of the southern South China Sea bounded within 98°E to 113°E and 0°S to 15°N (Figure 2), which includes the Gulf of Thailand and the Sunda Shelf. The bathymetry data was taken from the ETOPO5 ($5' \times 5'$) digital dataset from National Geophysical Data Centre (NGDC 2009) and bilinearly interpolated to the model grids with the resolution of $0.1^\circ \times 0.1^\circ$. A no-slip condition was applied for the model's closed boundaries and radiation type lateral boundary conditions were used for the open boundaries. The integration time step was set to 15 s and the atmospheric forcing was updated daily. The model was started cold where the initial value of SSE and depth integrated velocities was set to zero. Tidal effect, steric effect, mean sea level rise, sea ice melting and local vertical crustal motion effect were not included in the simulations to avoid complication.

SIMULATION OUTPUT ANALYSIS

For each grid point of model domain, the maximum SSE and wind speed values for each year were extracted and averaged to obtain the mean annual maximum SSE (surge height) and mean annual maximum wind speed, respectively. The comparison of wind speed and surge height between the hindcast and baseline simulations, and baseline and future simulation were then performed. In current study, only the wind speed was selected for the climate change extreme analysis instead of the atmospheric pressure. According to depth-averaged hydrodynamic equation, the wind stress forcing term is divided by the total depth of water whereas the atmospheric pressure forcing term is not divided by depth (Flather 2001). Hence, surface wind speed is more relevant in driving the storm surge over the shallow seas. This statement is further supported by Cerrère and Lyard (2003) in their barotropic model experiments, showing that the ocean response to atmospheric pressure is much weaker compared to the atmospheric wind forcing. In other words, wind forcing

TABLE 1. List of selected stations and its location. Years of data are the years used in finding the range of natural variability in observed data (Figure 3). RMSEs are computed for year 1987-1989 between the simulated hourly mean sea level elevations of ERA40 with observations at selected stations

| Station | Name of stations | Location | Year | 1987-1989 |
|---------|------------------|-------------------|-------------|-----------|
| | | | | RMSE (cm) |
| 1 | Pulau Tioman | 2.48°N, 104.08°E | 1986 – 2006 | 10.272 |
| 2 | Kuantan | 3.59°N, 103.26°E | 1984 – 2006 | 10.648 |
| 3 | Cendering | 5.16°N, 103.11°E | 1985 – 2006 | 11.979 |
| 4 | Geting | 6.14°N, 102.06°E | 1987 – 2006 | 15.033 |
| 5 | Kolak | 11.48°N, 99.49°E | 1985 – 2009 | 13.743 |
| 6 | Vungtau | 10.20°N, 107.04°E | 1986 – 2002 | 14.621 |

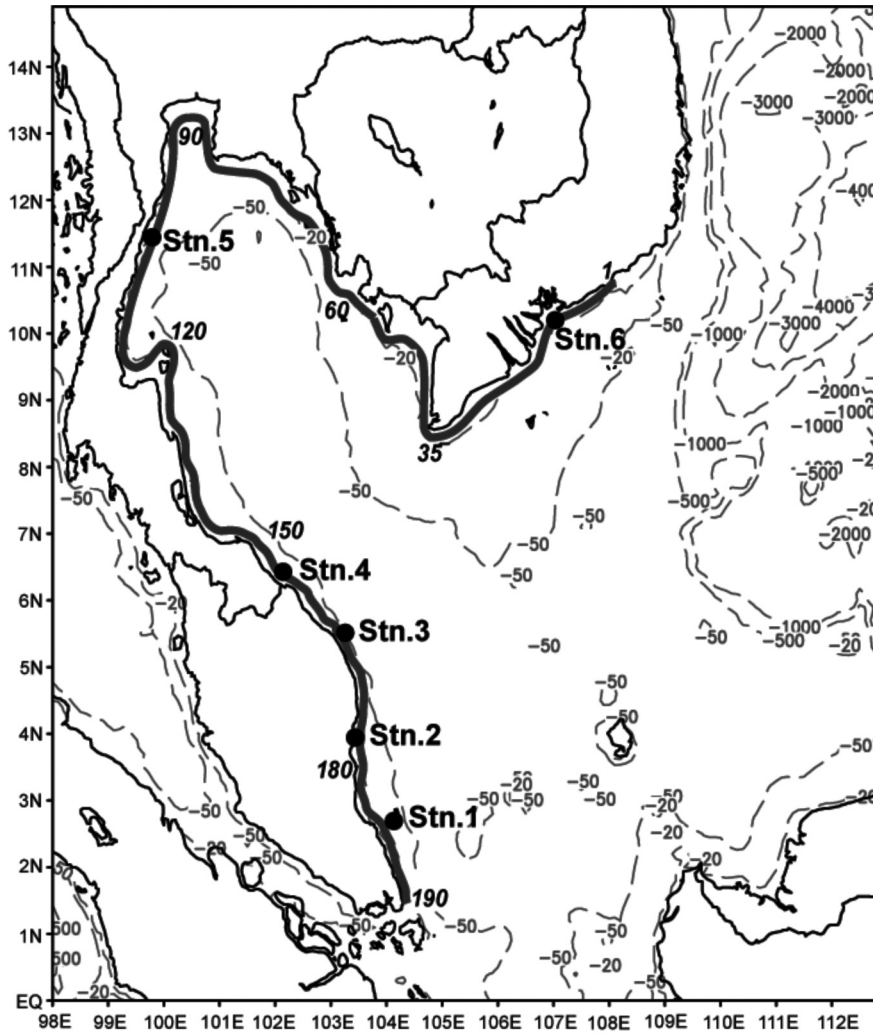


FIGURE 2. Model domain and location of the selected stations for model validation. Bold italic numbers represent the number of grid point along the coastline (thick grey line). Grey dashed lines indicate the bathymetry

become relatively more important than pressure as the water gets shallows.

The Generalized Extreme Value (GEV) distribution with the derivative of its probability density function given below (equation 3) (Butler et al. 2007; Huang et al. 2008; Sterl et al. 2009) is fitted to the annual maximum surge height (y):

$$G(y; \mu, \sigma, \xi) = \exp \left\{ - \left[1 + \xi \left(\frac{y - \mu}{\sigma} \right) \right]^{\frac{1}{\xi}} \right\}. \quad (3)$$

The three parameters represent the location (μ), the scale (σ) and the shape (ξ) of the distribution curve. The GEV combines three types of distribution model that include the Gumbel ($\xi = 0$), Weibull ($\xi < 0$) and Frchet ($\xi > 0$) distribution. The parameters were determined by using the maximum likelihood estimation (MLE) method. The fitted distribution was used to obtain the surge height estimation at return period of 5-year, 10-year and 50-year, respectively, along the coastline of the study domain (grey

thick line in Figure 2). The return level, $L(T_r)$ for a certain return period, T_r is computed as:

$$L(T_r) = G^{-1} \left(1 - \frac{1}{T_r} \right). \quad (4)$$

The return level for the selected return period was compared between the hindcast, baseline simulation and the future simulation. A Wilcoxon rank sum test (Debernard et al. 2002; Lowe et al. 2001; Wilks 2006) was used to examine significant changes in the extreme surge climate in the future.

RESULTS AND DISCUSSION

MODEL VALIDATION

The strength and limitation of POM were examined by comparing the simulated hourly SSE forced by ERA40 (hindcast) with the station observations. Due to the temporal limitation of the observed data, the simulated

SSE was compared with the chosen stations only for the available common year from 1987-1989. The hindcast downscaling simulation captured the annual fluctuation of the SSE reasonably well with a weaker magnitude (Figure 3). A lower SSE was simulated during the Northeast monsoon (November-March) while a slightly higher SSE values were simulated during the Southwest Monsoon. The annual fluctuation in simulated SSE was associated with the net flow toward the west coast of Sunda Shelf during northeast monsoon and water flow away during southwest monsoon (Morimoto et al. 2000). For a better

comparison, the root mean squared errors (RMSE) for SSE between the observations and the simulations were computed (Table 1). Stations located at the southeastern coast of Peninsular Malaysia (Stations 1 and 2) showed more consistent simulation with lower RMSE values. In general, the model simulates the SSE reasonably well with both the hindcast and baseline SSE annual cycles (1961-1990) fluctuate within the ranges of observed SSE in all of the examined stations (Figure 4).

The SSE biases between the simulation and the observation may be resulted from several possible causes.

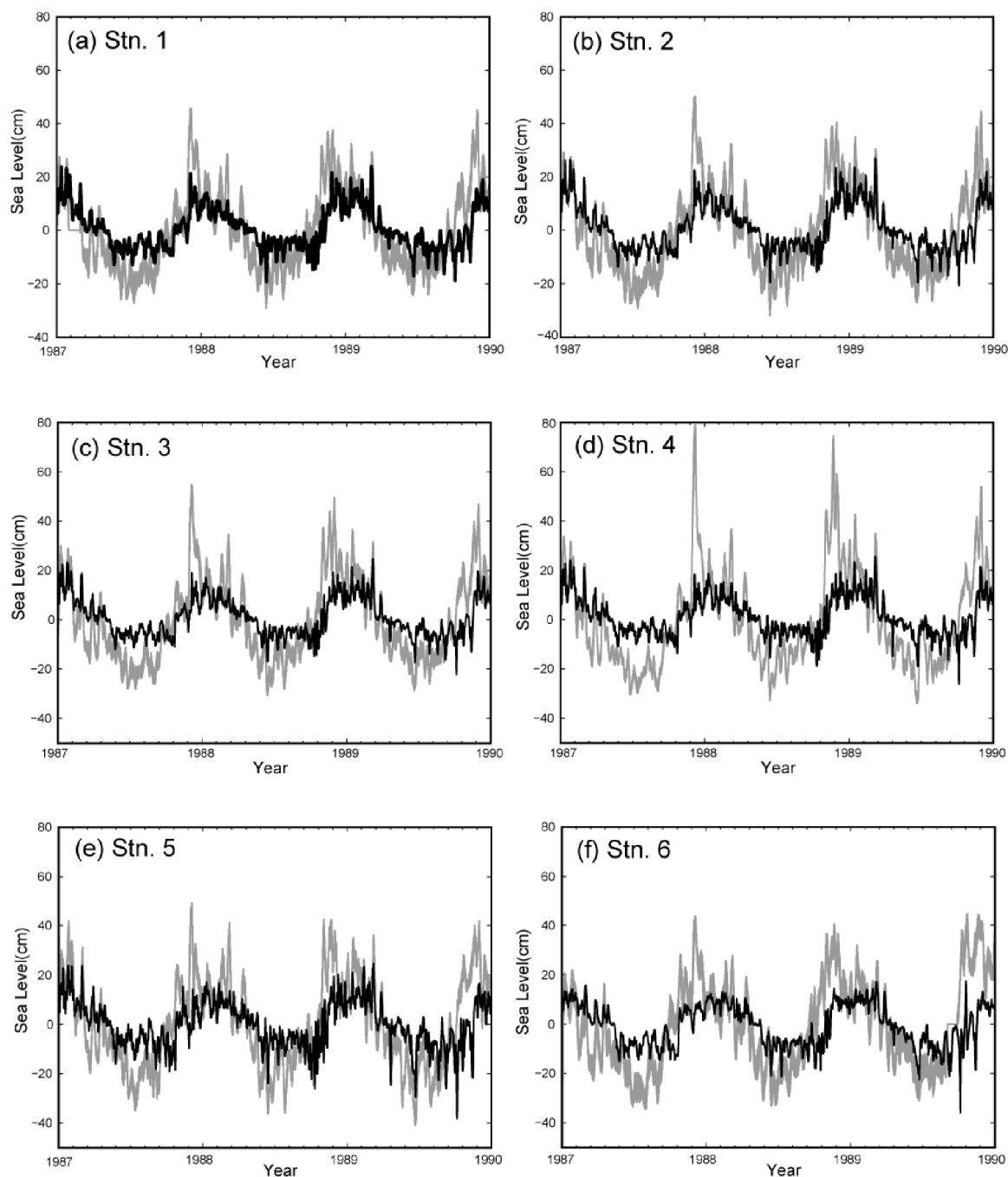


FIGURE 3. Hourly sea level elevations at six selected stations from year 1987-1989. Grey line indicates observation and black line indicates the simulated sea level elevations

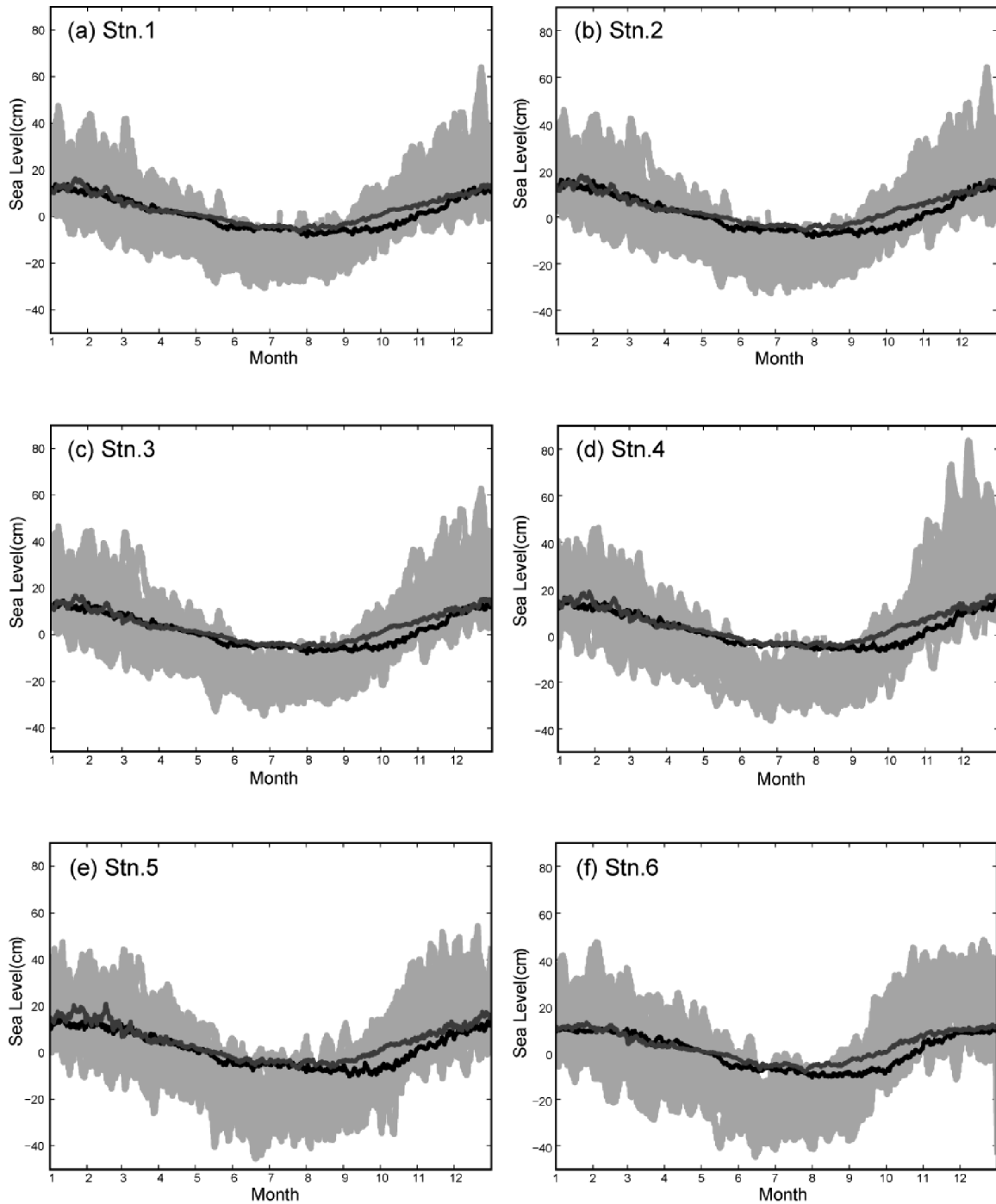


FIGURE 4. Annual cycle of sea level elevation for hindcast (black thick line) and baseline simulation (dark grey thick line). The light grey shaded areas represent the range of sea level elevation derived from the observation

The exclusion of the tide effect from the experiments results in the absence of non-linear interactions between the wind-forced surges with the tidal components. This may incur significant errors in the simulations. As an important driver, the atmospheric wind input largely governs the quality of the simulation result of the South China Sea circulation (Metzger 2003). The inadequacy of model to reproduce the high peaks values may arise from the weaker wind output from the RCM which the storm surge

extremes simulation is sensitive to. The lower temporal resolution (daily) of the atmospheric forcing may reduce the variance of simulated SSE (Zhuang et al. 2010). In addition, the deficiencies of model may also attribute to the comparison of grid averaged value with a single point observed value. In addition, the large biases in SSE may also induced by the ocean model inadequacy in simulating the Ekman dynamics in the study region. Since the study focuses on the changes of the surge climate rather than the

absolute values of the surge height, the simulations can still be useful to provide some insight to the evolution of storm surge under the possible future climate change scenario.

HINDCAST VS BASELINE SIMULATIONS (1961-1990)

The historical climate for the averaged annual maximum wind speed and surge height derived from the hindcast simulation are shown in Figures 5(a) and 5(b), respectively. The wind speed gradient was higher along the coastlines while the averaged annual maximum wind speed ranged from 2 m s^{-1} to 18 m s^{-1} , decreasing from the northeast toward southwest and the central of the Gulf of Thailand. High averaged annual maximum wind speed was found over east of Vietnam coast and this can be attributed to the orographic effect of Annam Cordillera mountain range (Xie et al. 2003). On the other hand, the averaged annual maximum surge height increased toward the Gulf of Thailand and the eastern coast of Peninsular Malaysia with the surge height ranged from 0 cm to 40 cm. However, slightly higher surges were found at the southeast of Vietnam coast. Interestingly, the general pattern of the historical surge height extreme bears resemblance to the distribution of the most dominant mode of the empirical orthogonal function (EOF) analysis of the intraseasonal variability of sea level in the Gulf of Thailand reported by Zhuang et al. (2010). This mode is characterized by the increasing amplitude from the mouth of the gulf toward the inner part. This suggests that the climate of the surge height extreme over the gulf is likely dominated by strong

intraseasonal variations. The intraseasonal variations are also clearly visible in Figure 3.

The SSE annual cycle of the baseline simulation was consistent with the hindcast values for all the stations with larger biases during the monsoon transition period (from the southwest monsoon to the northeast monsoon). The wind field was weaker and less consistent during the monsoon transition period compared with the monsoon seasons. Baseline simulation showed an earlier SSE phase changes (from negative to positive) compared with those of the hindcast SSE climate. The spatial distributions of differences for the annual maximum wind speed and surge height of the two simulations are shown in Figure 6. Negative biases were found in the annual maximum wind speed while positive biases were apparent in the simulated surge height in the Gulf of Thailand. Weaker wind speed was found in the inner part of the Gulf of Thailand, Malacca Strait, Karimata Strait and offshore of east Vietnam. However, the positive biases of the surge height indicates higher surge in the baseline simulation that was likely associated to the wind orientation rather than the wind speed. The annual maximum wind direction was suspected to direct towards land and causing a positive biases in surge height although the maximum wind speed was weaker in baseline simulation.

The comparison of SSE annual extreme return levels between the hindcast and baseline simulation for the 5-year, 10-year and 50-year return period is shown in Figure 7. The grid numbers on the abscissa represent the grid boxes, numbered from 1 to 190, along the coastline

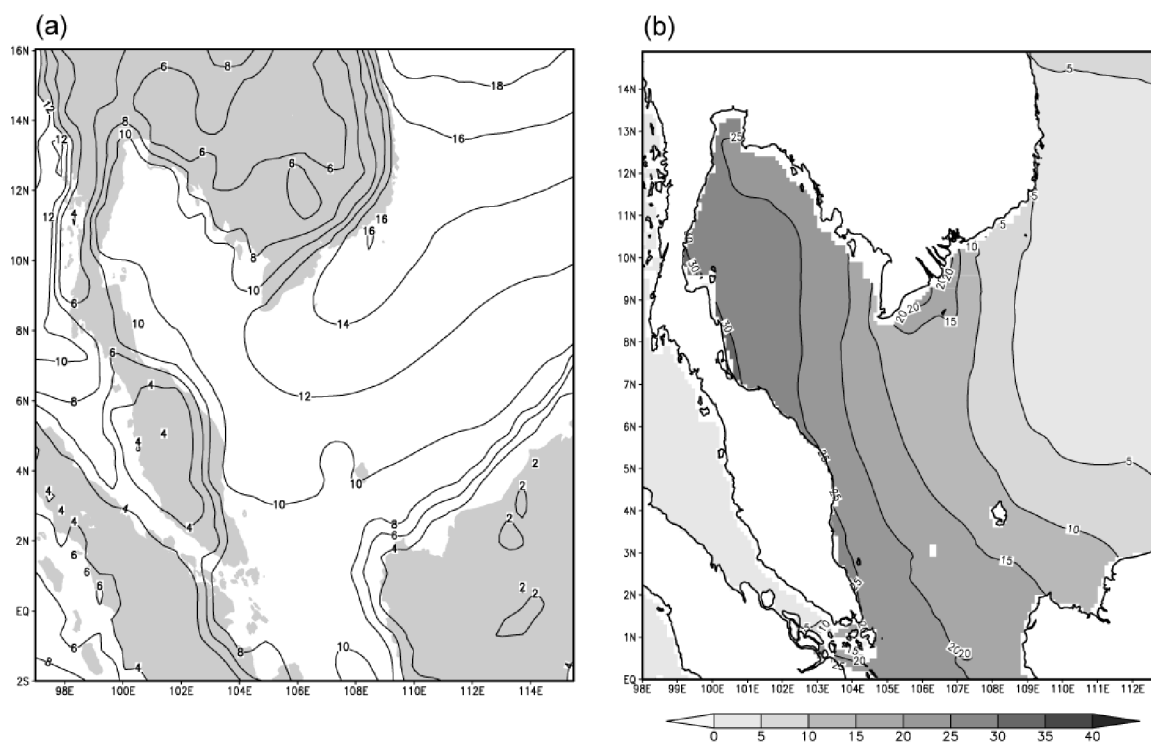


FIGURE 5. The historical climate for annual maximum wind speed (5(a); unit: ms^{-1}) and annual maximum surge height (5(b); unit: cm) derived from hindcast simulations for 1961-1990

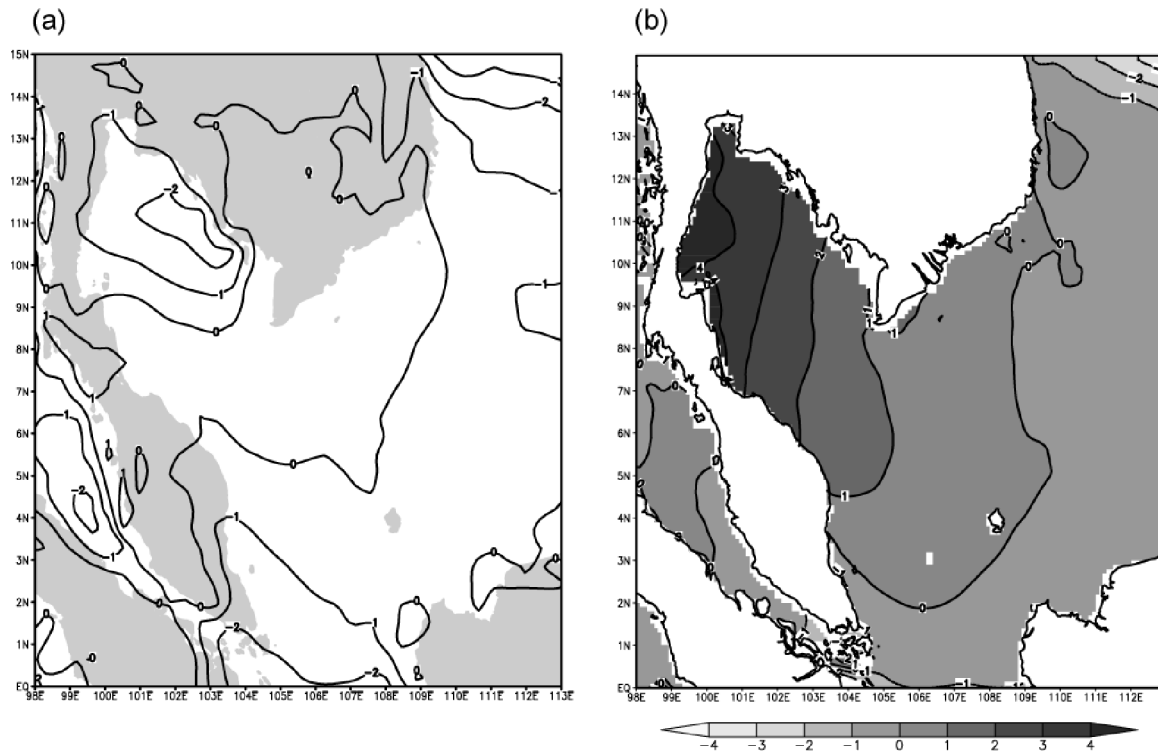


FIGURE 6. Biases of the averaged annual maximum wind speed (6(a); unit: ms^{-1}) and annual maximum surge height (6(b); unit: cm) from the baseline and hindcast from 1961-1990

of the Sunda Shelf as shown in Figure 2 (grey thick line). The return levels for three return periods showed similar trends along the coastline. The extreme surge return levels increase towards the inner coast of the Gulf of Thailand (started from grid point 60) and decreased as it moves toward the southern coast of the Sunda Shelf. The return levels along the coastline of Vietnam (grid point 1-60) and southeast coast of Peninsular Malaysia (grid point 160-190) in the baseline simulation were consistent with the hindcast simulation. However, the baseline simulation always have higher estimates of return levels of the extreme surge along the coastline around the Gulf of Thailand (Grid point 70-150) compared with hindcast simulation. The deviation may be caused by the differences in the strength of wind forces used in the simulation. The baseline extreme return level deviates more from the hindcast in the shorter return period. Higher return level was obtained as the return period increases. Generally, the baseline simulation was consistent with the hindcast simulation where the return levels reproduced lie within the 95% confident interval derived from hindcast simulation for all the three considered return periods.

FUTURE CLIMATE PROJECTION (2071-2100)

For the climate projection analysis of the storm surge, the differences between the baseline climate and the SRES A2 scenario projection were expressed as the relative changes of present-day statistics in the projected future. The percentage changes of the annual maximum wind speed

and surge height under the SRES A2 scenario are shown in Figure 8. The spatial pattern of wind speed percentage changes (Figure 8(1)) suggests increasing wind speeds along the coastline of the western Gulf of Thailand and Peninsular Malaysia. Larger percentage changes were found over the Peninsular Malaysia, western Borneo and southern tip of Thailand. These changes were statistically significant at 5% level using the Wilcoxon rank sum test. Most of the percentage of wind speed changes over the landmass was significant at 5% level. Moreover under the SRES A2 emission scenario, the wind speeds over the open marine environment are predicted to decrease with largest decrement about 5% occurs over the area off coast of east Vietnam.

On the other hand, the maximum annual surge extreme was expected to increase $\sim 5\text{-}20\%$ over the western coast of the Gulf of Thailand (Figure 8(b)). For the coastline along the Peninsular Malaysia, the surge extremes were predicted to increase by $\sim 10\%$ in the southeastern part and by $\sim 15\%$ in the western coast. The changes of surge extreme were proportional to the changes of wind speed with higher increment in wind speed induces higher surge extreme in the future SRES A2 emission scenario. Significant decrements up to $\sim 45\%$ in surge height were expected in the offshore of southeast Vietnam. The minimal and insignificance of wind speed changes in this area indicated that the decrease surge height may be induced by other factors such as the increasing of baroclinic effect over the deep basin. In general, it can be concluded that the

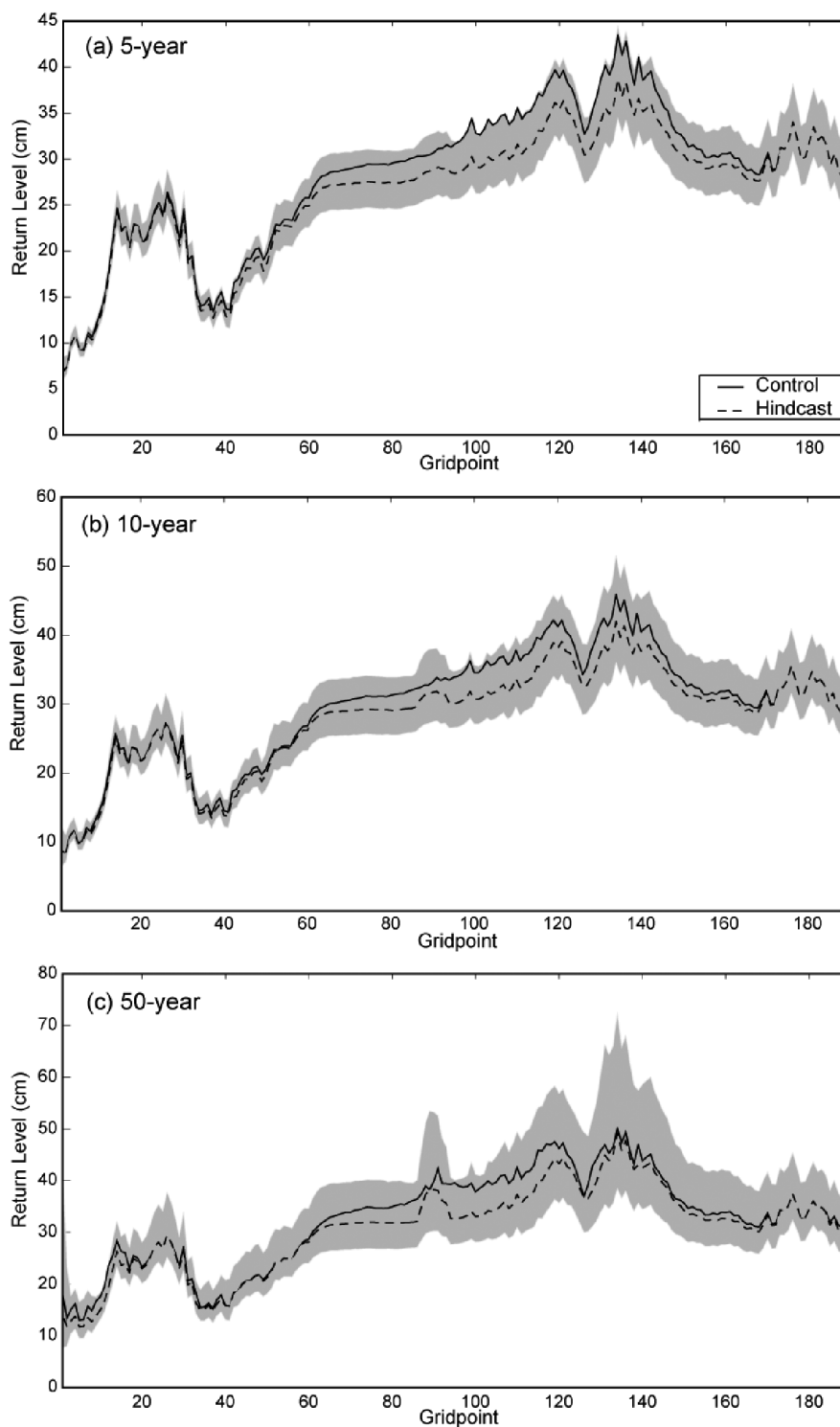


FIGURE 7. Return levels of extreme surge height for a) 5-year, b) 10-year and c) 50-year return period. Solid line represents the baseline simulation and dotted line represent the hindcast simulation from year 1961-1990. The grey-shaded bands represent the 95% confidence interval of the natural variability derived from hindcast simulation

predicted changes of surge extreme in future are induced by the changes of regional wind speed under the increasing greenhouse gases scenario over the shallow regions.

The changes of the 5 year, 10 year and 50 year surge extreme return levels were also examined (Figure 9). The

result suggested that there are increasing 5 year, 10 year and 50 year surge extreme return levels along the coastline of Sunda Shelf. Nevertheless, the distribution of surge extreme changes may differ geographically. The surge extreme return levels for the three return periods were

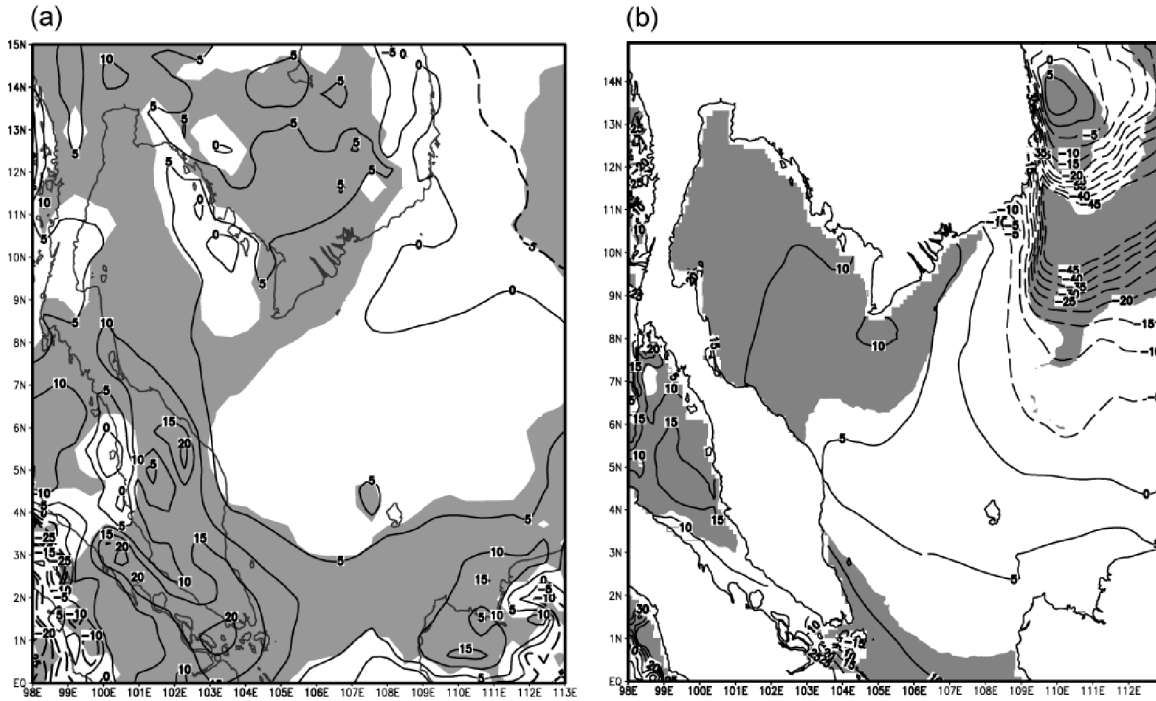


FIGURE 8. The percentage changes of annual maximum wind speed (8(a)) and surge height (8(b)) (A2-BL) in future emission scenario. Contours represent the changes and grey-shaded areas represent the significance of changes

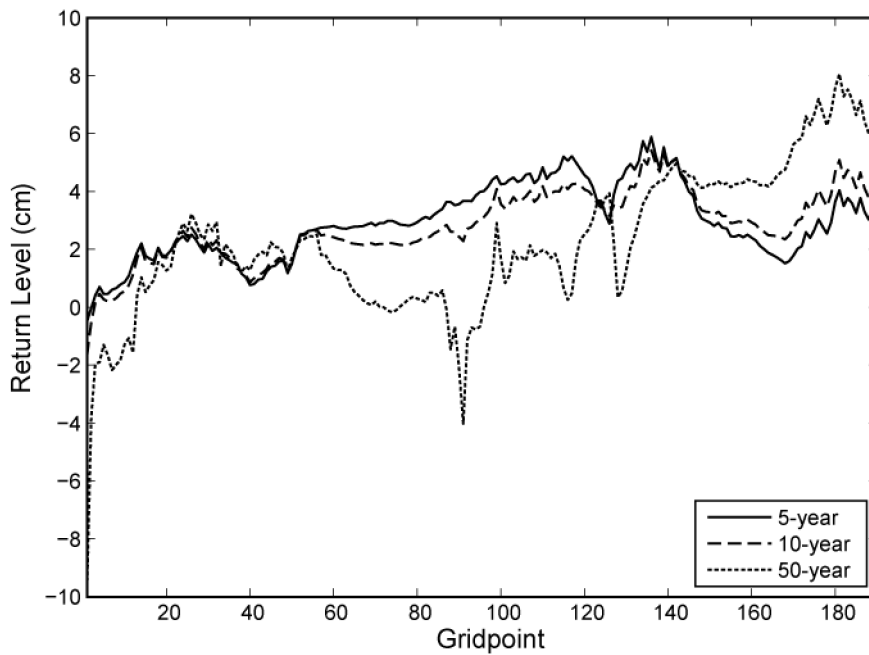


FIGURE 9. The changes of return level for extreme surge height between baseline and future simulation (A2-BL)

rather small around the coast of Vietnam and Cambodia (grid point 10-60). However, larger changes (7-14%) in the 5-year and 10-year return levels were projected along the coastline of Gulf of Thailand. Along the coast of Peninsular Malaysia, the 50 year return levels show larger increment of ~20% as compared with the weaker

increment of 5 year and 10 year return levels. In general, the frequencies of surge extreme along the coastline of Sunda Shelf were projected to increase under the future warmer climate primarily due to modification of regional surface wind characteristics associated with the warming.

CONCLUSION

A two dimensional barotropic storm surge model was configured to simulate the sea level elevation for present day (1961-1990) and future (2071-2100) climate condition. The atmospheric forcings data was taken from a regional climate model output - PRECIS which dynamically downscale the baseline climate and the SRES A2 scenario climate simulation from the MPI's ECHAM4. The model result was compared with the SSE from the hindcast simulation forced by downscaled ERA40 and also with the stations observation. The simulations reproduce the surge climate satisfactorily despite biases in the magnitude of the variations. In the projected climate, the distribution of surge extreme changes is inhomogeneous over the considered domain. Significant changes are found over the Gulf of Thailand and southeast coast of Peninsular Malaysia. The projection of storm surges shows a small change surge extreme in response to the atmospheric wind change. The surge extreme is projected to increase by ~9% overall with a ~5% of stronger wind speeds over the Sunda Shelf. In the return level analysis, the changes of surge extreme at certain return period shows considerable spatial variations. Shorter term (5 and 10 year) return levels are expected to increase more along the coast of Gulf of Thailand whilst the long term (50 year) return levels increase more along the eastern coast of Peninsular Malaysia. The result indicates that the regions along the Sunda Shelf coastline areas can be vulnerable and may be susceptible to increase surge hazards forced by large and regional scale atmospheric changes.

Despite encouraging results, this study reveals some caveats. The current study is still inadequate to provide a good estimation of extreme sea level for local adaptation measures such as the coastal defenses and management around the Sunda Shelf coastlines. The exclusion of non-linear interaction between the surge and the tide effect may reduce the magnitude of the seasonal variation in the simulations. While it can serve as a preliminary examination of the possible alteration of surge extreme climate caused by global warming, future study may consider improved driving atmospheric forcings and finer model grid resolution for less-biased simulation. Hence, careful handling is required for any downstream utilization of current modeling result. The fact that model failed to reproduce the extreme tails of the historical SSE hampers the confident estimation of the changes magnitude. However, the sign of the chances should still be valid. In addition, a single climate scenario is insufficient for the estimation of the uncertainties in the future projection. The response of the surge model to different emission scenarios and driving by different regional climate models output is required to quantify the uncertainties in the extreme surge climate projections.

ACKNOWLEDGEMENT

This research was funded by Universiti Kebangsaan Malaysia Research University Grants UKM-AP-PI-18-2009/2 and LRGS/TD/2011/UKM/PG/01.

REFERENCES

- Ascharyaphotha, N., Wongwises, P., Humphries, U.W. & Wongwises, S. 2011. Study of storm surge due to Typhoon Linda (1997) in the Gulf of Thailand using a three dimensional ocean model. *Applied Mathematics and Computation* 217: 8640-8654.
- Bell, R.G., Goring, D.G. & de Lange, W.P. 2000. Sea level change and storm surges in the context of climate change. *IPENZ Transactions* 27: 1-10.
- Bernier, N.B. & Thompson, K.R. 2006. Predicting the frequency of storm surge and extreme sea levels in the northwest Atlantic. *Journal of Geophysical Research* 111: C10009.
- Blumberg, A.F. & Mellor, G.L. 1983. Diagnostic and prognostic numerical circulation studies of the South Atlantic Bight. *Journal of Geophysical Research* 88: 4579-4592.
- Burnett, W.H., Kamenkovich, V.M., Jaffe, D.A., Gordon, A.L. & Mellor, G.L. 2000. Dynamical balance in the Indonesian seas circulation. *Geophysical Research Letters* 27: 2705-2708.
- Butler, A., Heffernan, J.E., Tawn, J.A., Flather, R.A. & Horsburgh, K.J. 2007. Extreme value analysis of decadal variations in storm surge elevations. *Journal of Marine Systems* 67: 189-200.
- Cerrère, L. & Lyard, F. 2003. Modeling the barotropic response of the global ocean to atmospheric wind and pressure forcing: Comparisons with observations. *Geophysical Research Letters* 30: 1275.
- Debernard, J., Saetra, Ø. & Røed, L.P. 2002. Future wind, wave and storm surge climate in the northern North Atlantic. *Climate Research* 23: 39-49.
- Flather, R.A. 2001. Storm surges. In *Encyclopedia of Ocean Sciences*, edited by Steele, J.H., Thorpe, S.A. & Turekian, K.K., San Diego: Academic Press.
- Gönnert, G. 2004. Maximum storm surge curve due to global warming for the European North Sea region during the 20th-21st century. *Natural Hazards* 32: 211-218.
- Hori, M. & Ueda, H. 2006. Impact of global warming on the East Asian winter monsoon as revealed by nine coupled atmosphere-ocean GCMs. *Geophysical Research Letters* 33: L03713.
- Hu, Z.-Z., Bengtsson, L. & Arpe, K. 2000. Impact of global warming in the Asian winter monsoon in a coupled GCM. *Journal of Geophysical Research* 105: 4607-4624.
- Huang, W., Xu, S. & Nanji, S. 2008. Evaluation of GEV model for frequency analysis of annual maximum water levels in the coast of United States. *Ocean Engineering* 35: 1132-1147.
- IPCC. 2007. *Climate Change 2007: The Physical Science Basis. Contribution of Working Group I to the Fourth Assessment Report of the Intergovernmental Panel on Climate Change*. Cambridge and New York: Cambridge University Press.
- Juneng, L. & Tangang, F.T. 2010. Long-term trends of winter monsoon synoptic circulation over the maritime continent: 1962-2007. *Atmospheric Science Letter* 11: 199-203
- Kolomiets, P., Zheleznyak, M. & Tklich, P. 2010. Dynamical downscaling of storm surges in South China Sea and Singapore Strait. *Storm Surge Congress 2010*. Germany: Harburg.

- Lionello, P., Nizzero, A. & Elvini, E. 2003. A procedure for estimating wind waves and storm-surge climate scenarios in a regional basin: The Adriatic Sea case. *Climate Research* 23: 217-231.
- Lowe, J.A., Gregory, J.M. & Flather, R.A. 2001. Changes in the occurrence of storm surge in United Kingdom under a future climate scenario using a dynamic storm surge model driven by Hadley Centre climate models. *Climate Dynamics* 18: 197-188.
- Mellor, G.L. 2004. *Users Guide for a Three-Dimensional, Primitive Equation, Numerical Ocean Model*. Princeton, New Jersey: Princeton University.
- Morimoto, A., Yoshimoto, K. & Tanagi, T. 2000. Characteristics of sea surface circulation and eddy field in the South China Sea revealed in satellite altimetric data. *Journal of Oceanography* 56: 331-344.
- Metzger, E.J. 2003. Upper ocean sensitivity to wind forcing in the South China Sea. *Journal of Oceanography* 59: 783-798.
- NGDC, 2009. ETOPO5 5-minute gridded elevation data. <http://www.ngdc.noaa.gov/mgg/global/etopo5.HTML>. Accessed 16 August 2009.
- Peng, M., Xie, L. & Pietrafesa, J. 2006. A numerical study on hurricane-induced storm surge and inundation in Charleston Harbors, South Carolina. *Journal of Geophysical Research* 111: C08017.
- Pittock, A.B., Walsh, K. & McInnes, K. 1996. Tropical cyclones and coastal inundation under enhanced greenhouse conditions. *Water, Air and Soil Pollution* 92: 159-169.
- PSMSL. 2010. The permanent service for mean sea level: Further information. <http://www.psmsl.org/data/obtaining/psmsl.hel>. Accessed 30 January 2010.
- Rupa Kumar, K., Sahai, A.K., Krishna Kumar, K., Patwardhan, S.K., Mishra, P.K., Revadekar, J.V., Kamala, K. & Pant, G.B. 2006. High-resolution climate change scenarios for India for the 21st century. *Current Science* 90: 334-345.
- Sheffield, J. & Wood, E.F. 2008. Projected changes in drought occurrence under future global warming from multi-model, multi-scenario, IPCC AR4 simulations. *Climate Dynamics* 31: 79-105.
- Sterl, A., van den Brink, H., de Vries, H., Haarsma, R. & van Meijgaard, E. 2009. An ensemble study of extreme storm surge related water levels in the North Sea in a changing climate. *Ocean Science* 5: 369-378.
- von Storch, H. & Woth, K. 2008. Storm surges: Perspectives and options. *Sustainability Science* 3: 33-43.
- Wannawong, W., Humphries, U.H. & Wongwiset, P. 2010. Numerical modeling and computation of storm surge for primitive equation by hydrodynamic model. *Thai Journal of Mathematics* 8: 355-371.
- Wilks, D.S. 2006. *Statistical Methods in the Atmosphere Sciences*. Boston: Academic Press.
- Wilson, S., Hassell, D., Hein, D., Jones, R. & Taylor, R. 2009. *Installing and using the Hadley Centre regional climate modeling system using PRECIS. Version 1.8.2*. Exeter: UK Met Office Hadley Centre.
- Woth, K., Weisse, R. & von Storch, H. 2006. Climate change and North Sea storm surge extremes: An ensemble study of storm surge extremes in a changed climate projected by four different regional climate models. *Ocean Dynamics* 56: 3-15.
- Xie, S.P., Xie, Q., Wang, D. & Liu, W.T. 2003. Summer upwelling in the South China Sea and its role in regional climate variations. *Journal of Geophysical Research* 108: 3261-3273.
- Zhuang, W., Xie, S.P., Wang, X., Taguchi, B., Aiki, H. & Sasaki, H. 2010. Intraseasonal variability in sea surface height over the South China Sea. *Journal of Geophysical Research* 11: 5C04010.

Research Centre for Tropical Climate Change System (IKLIM)
Faculty of Science and Technology
Universiti Kebangsaan Malaysia
43600 Bangi, Selangor D.E.
Malaysia

*Corresponding author; email: juneng@ukm.my

Received: 30 April 2012

Accepted: 27 June 2012